# Accepted Manuscript

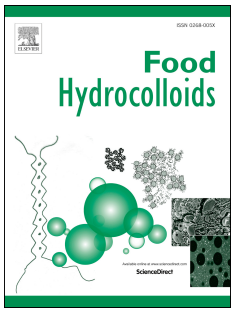


Bioactive starch nanocomposite films with antioxidant activity and enhanced mechanical properties obtained by extrusion followed by thermo-compression

Santiago Estevez-Areco, Lucas Guz, Lucía Famá, Roberto Candal, Silvia Goyanes

PII: S0268-005X(19)30607-1

DOI: https://doi.org/10.1016/j.foodhyd.2019.05.054

Reference: FOOHYD 5153

To appear in: *Food Hydrocolloids*

Received Date: 27 March 2019

Revised Date: 27 May 2019

Accepted Date: 30 May 2019

Please cite this article as: Estevez-Areco, S., Guz, L., Famá, Lucí., Candal, R., Goyanes, S., Bioactive starch nanocomposite films with antioxidant activity and enhanced mechanical properties obtained by extrusion followed by thermo-compression, *Food Hydrocolloids* (2019), doi: https://doi.org/10.1016/j.foodhyd.2019.05.054.

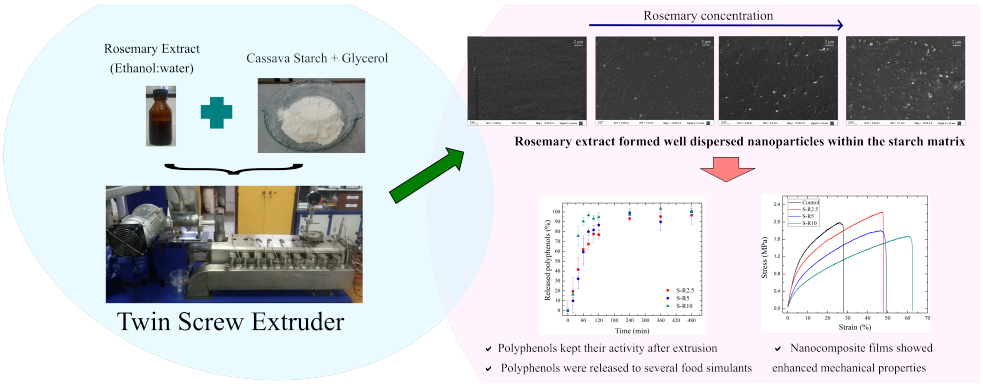

# Bioactive starch nanocomposite films with antioxidant activity and enhanced mechanical properties obtained by extrusion followed by thermo-compression

Santiago Estevez-Areco[a], Lucas Guz[a], Lucía Famá[a], Roberto Candal[b*], Silvia Goyanes[a*]

[a]Universidad de Buenos Aires, Facultad de Ciencias Exactas y Naturales, Departamento de Física, Laboratorio de Polímeros y Materiales Compuestos (LP&MC), Instituto de Física de Buenos Aires (IFIBA-CONICET). Ciudad Universitaria (1428), Ciudad Autónoma de Buenos Aires, Buenos Aires, Argentina.

[b]Instituto de Investigación e Ingeniería Ambiental, CONICET, Universidad Nacional de San Martín. Campus Miguelete, 25 de mayo y Francia, San Martín (1650), Pcia. Buenos Aires, Argentina.

*Corresponding authors: rcandal@unsam.edu.ar; goyanes@df.uba.ar

## Abstract

In this work bioactive starch films with antioxidant activity were developed by extrusion followed by thermo-compression. Rosemary extract was incorporated into starch-glycerol films in different concentrations (2.5%, 5% and 10% w/w with respect to starch). Despite the high mechanical and thermal energy involved during extrusion, rosemary polyphenols remained in the films without losing its activity.

Starch nanocomposites were obtained by the incorporation of rosemary nanoparticles, which were formed from the immiscible components of the extract. For low extract concentration, homogeneously dispersed nanoparticles acted as reinforcement of the matrix, increasing stress and strain at break without modifying Young's modulus. At high concentration, the mechanical response was ruled by the miscible components of the extract, which acted as an additional plasticizer. In this case, nanocomposite films with higher values of strain at break and lower values of Young's modulus and stress at break were obtained. All the developed films released a high percentage of polyphenols to hydrophilic, lipophilic or acid food simulants in a short time interval. Experimental release data was fitted by Weibull equation in order to elucidate release mechanisms.

According to the results of this research, rosemary extract can be incorporated into starch films by extrusion without previous encapsulation. Despite thermal and mechanical energy involved in the process, the rosemary compounds kept their antioxidant activity and were released from the bioactive films.

*Keywords*: Bioactive starch films; Extrusion; Rosemary extract; Antioxidant activity; Release kinetics; Mechanical properties.

# 1. Introduction

The development of biodegradable and bio-based materials – obtained from polysaccharides, proteins or lipids, for example - is a field of growing interest around the world since they help to mitigate the environmental problems caused by the use of fossil derived polymers. The food-packaging industry in particular contributes around 40% of worldwide plastic production (IHS Markit, 2018). The replacement of conventional packaging with biodegradable and bio-based materials is also a central issue for environmental care. In this context, polysaccharide films are one of the most studied systems at present (Cazón, Velazquez, Ramírez, & Vázquez, 2017). Starch is a promising alternative as a base component for food packaging applications due to its ready availability, low cost, biodegradability, and because it is a great film forming biopolymer (García, Famá, D'Accorso, & Goyanes, 2015; Shah, Naqash, Gani, & Masoodi, 2016). Incorporation of functional compounds into starch films for food packaging applications constitutes an interesting approach to extend the shelf life of food products, by preventing microbial growth or oxidative damage (Guz, Famá, Candal, & Goyanes, 2017; Khaneghah, Hashemi, & Limbo, 2018; Vilela et al., 2018; Yildirim et al., 2018). Natural bioactive components are generally regarded as safe (GRAS) (US Food & Drug Administration, 2018) and they are preferred by consumers over synthetic ones, which are frequently associated with health and environmental problems.

Several researches have focused on the incorporation of natural extracts or essential oils to starch films and their effects on the physical, chemical and active properties of the obtained material (dos Santos Caetano et al., 2018; Feng et al., 2018; Iamareerat, Singh, Sadiq, & Anal, 2018; Ortega-Toro, Collazo-Bigliardi, Roselló, Santamarina, & Chiralt, 2017). In particular, rosemary (*Rosmarinus officinalis*) extracts constitute an important source of bioactive compounds with important antioxidant activity. Previously, our group has reported the incorporation of different rosemary extracts into starch films. An aqueous rosemary extract led to an improvement in UV-blocking properties and an increase in the hydrophobicity of starch films (Piñeros-Hernandez, Medina-Jaramillo, López-Córdoba, & Goyanes, 2017), while an ethanol based rosemary extract led to the formation of rosemary nanoparticles within the matrix, which acted as a mechanical reinforcement (López-Córdoba, Medina-Jaramillo, Piñeros-Hernandez, & Goyanes, 2017).

However, these bioactive materials were obtained by casting technique, as is done in most of the studies related to starch active films. Scalable techniques such as extrusion are a necessity in the field of materials science in order to make starch films implementation feasible on an industrial scale. Extrusion is suitable to set a large-scale production of starch films via a continuous process that employs low amount of water, high temperature and shear forces to gelatinize the starch granules (Ji et al., 2017). Nevertheless, the obtained materials differ in their physical properties from those obtained by casting (Ochoa-Yepes, Di Giogio, Goyanes, Mauri, & Famá, 2019). For the development of active films, mechanical and thermal energy could lead to the loss or diminution of activity of the incorporated compounds (Domínguez et al., 2018). For example, it was recently reported that pH-sensitive nanoclays (montmorillonite containing *Jamaica flower* anthocyanins or blueberry extract) were exfoliated during extrusion of starch, which led to the thermal degradation of the encapsulated compounds (Gutiérrez, Herniou-Julien, Álvarez, & Alvarez, 2018; Toro-Márquez, Merino, & Gutiérrez, 2018).

Rosemary extracts present high thermal stability, without significant mass losses until 190 °C (Cordeiro et al., 2013), which suggests that active compounds could resist the high temperatures employed during starch extrusion (usually below 150 °C) without previous encapsulation. Additionally, rosemary extract granted a high antioxidant activity to starch films developed by casting, and its presence improved its physicochemical characteristics (López-Córdoba et al., 2017; Piñeros-Hernandez et al., 2017).

The aim of this work was the development of bioactive nanocomposite films by extrusion followed by thermo-compression from cassava starch containing rosemary extract, maintaining its high antioxidant capacity at the end of the manufacturing process. The employed rosemary extract showed the ability to form nanoparticles, and its effect over the physicochemical characteristics of the obtained films was studied. Antioxidant activity and release kinetics of rosemary polyphenols in different food simulants were evaluated in order to potentially use the obtained films as an active packaging.

## 2. Material and Methods

### 2.1 Materials

Cassava Starch (18% amylose ~1.5 x $10^5$ g/mol, 82% amylopectin ~$10^8$ g/mol) was supplied by Cooperativa Agrícola e Industrial San Alberto Limitada (C.A.I.S.A., Misiones, Argentina). Rosemary leaves were acquired in a local trade (Buenos Aires, Argentina). Analytical grade glycerol (Sigma-Aldrich, Germany), distilled water, Folin-Ciocalteu reagent (Anedra, Argentina), gallic acid (Biopack, Argentina), 2,2-diphenyl-1-picrylhydrazyl (DPPH) reagent (Sigma-Aldrich, Germany), Trolox (Sigma-Aldrich, Germany), methanol 99.8% and commercial grade ethanol 96% were used.

### 2.2 Rosemary extract

Ethanol based rosemary extract was prepared as previously reported (Estevez-Areco, Guz, Candal, & Goyanes, 2018). For its preparation, milled dried rosemary leaves (100 g) were immersed in 500 mL of ethanol:water solution (70:30 v/v) for 55 min at 50 °C. The extract was cooled at room temperature and filtered (pore size of 0.45 µm). Afterwards, it was dried in two steps: first with a rotary evaporator (DragonLab 100 Pro, USA) until its volume was reduced by a factor of 10 (50 rpm, 35°C), and then placed in a stove at 50 °C until a constant weight was reached. After that, a fine powder of rosemary extract was obtained. The powder rosemary extract was immediately used to prepare the mixtures for extrusion.

A turbid solution was obtained when the powder extract was dispersed in water (Section 2.3.1). This could be consequence of the formation of particles from the non-water soluble components of rosemary powder. In order to study these particles size and their composition, powder extract was dispersed in water at the highest ratio used to prepare the extrusion mixtures (15% w/w) and sonicated for 30 min. Size of rosemary particles was studied by SEM and the composition of the soluble and non-soluble phases were studied by HPLC-MS.

A drop of the dispersion was air dried at 50 °C, sputtered with a thin layer of platinum and examined by scanning electron microscopy (SEM) using a field emission gun Zeiss SUPRA 40.
Then, the dispersion was ultracentrifugated ($10^4$ rpm, 15 min) and the supernatant was collected. The precipitates were dissolved in ethanol (99.8%) and collected. Composition of supernatant and precipitates was studied by High Performance Liquid Chromatography (HPLC) using a Dionex UltiMate 3000 (Thermo Scientific) coupled to a LTQ XL mass spectrometer (Thermo Scientific) via an electrospray interface. The column used was a Hypersil Gold column (50 mm × 2.1 mm, d.p. 1.9 m) (Thermo Scientific) and the mobile phases consisted of ACN (0.1 formic acid, A) and water (0.1% formic acid, B) eluted according to the following gradient: 0 min, 95% B; 0.52 min, 95% B; 5.25 min, 40% B; 9.30 min, 5% B; 9.75 min; 5% B; 10.5 min, 95% B; 13.5 min, 95% B. Flow rate was 0.3 mL/min and the injection volume was 5 µL. The mass spectrometer was operated in the negative ESI multiple reaction monitoring (MRM). The values corresponding to the tube lens and collision energy were chosen according to Herrero, Plaza, Cifuentes, & Ibáñez (2010) in order to identify rosmarinic acid, carnosol and carnosic acid.

### 2.3 Films fabrication

#### *2.3.1 Mixtures preparation*

Mixtures of starch, glycerol and water were prepared according to González-Seligra, Guz, Ochoa-Yepes, Goyanes,& Famá (2017). Different amounts of rosemary extract (0%, 2.5%, 5.0%, and 10.0% w/w of starch) were incorporated in order to obtain four different systems. Rosemary extract was first dispersed in distilled water and sonicated for 30 min. Glycerol was added to this dispersion and it was incorporated into the powder starch. Mixtures were placed in an automatic mixer for 1 h, sieved with a mesh (2 mm) and stored for 24 h in sealed containers. Compositions and nomenclatures are summarized in Table 1.

Table 1: Nomenclature and composition of the different mixtures.

| Nomenclature | Starch (%) | Glycerol (%) | Water (%) | Rosemary extract (%) | Starch:Glycerol:Water ratio | Rosemary extract with respect to starch (%) |
|---|---|---|---|---|---|---|
| Control | 60.0 | 20.0 | 20.0 | 0.0 | 3:1:1 | 0.0 |
| S-R2.5 | 59.1 | 19.7 | 19.7 | 1.5 | 3:1:1 | 2.5 |
| S-R5 | 58.3 | 19.4 | 19.4 | 2.9 | 3:1:1 | 5.0 |
| S-R10 | 56.6 | 18.9 | 18.9 | 5.7 | 3:1:1 | 10.0 |

### *2.3.2 Extrusion process*

The extrusion of the different mixtures was carried out using a co-rotating twin screw extruder (Nanjing Kerke Extrusion equipment Co., Ltd., Jiangsu, China) with screw diameter of 16 mm, length of 640 mm and cylindrical die of 6 mm. Screw speed (80 rpm) and temperature profile (90-100-110-120-120-130-130-140-130-120 °C, from the feeder to the die) were selected in order to obtain a complete gelatinized material (González-Seligra et al., 2017). After extrusion, the thermoplastic threads were used to prepare films by thermo-compression using a thermo-stated hydraulic press. A piece of thread (~4 g) was placed between Teflon sheets and heated to 130 °C for 15 min. Pressure was then increased to 45 kPa and maintained for 15 min. Finally, temperature was decreased to room temperature while keeping the pressure. The resultant films were stored for 4 weeks at relative humidity of 56 % before tests, according to Morales, Candal, Famá, Goyanes, & Rubiolo (2015).

## 2.4 Characterizations

### *2.4.1 Morphological characterization*

Morphology of cryogenic fracture surface of the different films was studied by Scanning Electron Microscopy (SEM) using a field emission gun Zeiss DSM982 Gemini (Germany). Samples were frozen and fractured under liquid nitrogen, added to a support and then sputtered with a thin layer of platinum before observation.

### *2.4.2 Susceptibility to water*

Moisture content (MC) was determined according to the standard method of the AOAC (Cunniff & Jee, 1995). Samples of each system ($m_w$~0.5 g) were dried in an oven at 100 °C for 24 h and then weighted ($m_d$). Moisture content was calculated as:

$$MC(\%) = 100 \times \frac{m_w - m_d}{m_w}. \qquad (1)$$

Experiments were carried out in triplicate.

Water solubility (WS) was determined as:

$$WS(\%) = 100 \times \frac{m_{si} - m_{sf}}{m_{si}}, \qquad (2)$$

where $m_{si}$ is the initial dry weight and $m_{sf}$ is final dry weight. Initial dry weight was determined by drying 1.6 cm diameter discs in an oven at 100 °C for 24 h. Final dry weight was obtained by submerging other discs with similar diameter in 50 mL of distilled water at room temperature for 24 h, which were then dried at 100 °C for 24 h. Results are expressed as the average of 6 measurements.

Water vapor permeability (WVP) of films was measured using a modified ASTM E96-00 procedure. Samples of the different films were placed in circular acrylic cells containing $CaCl_2$ and located in desiccators at relative humidity (RH) of 70 % at room temperature. The cells weight was measured for 10 consecutive days, and the water vapor transport (WVT) was determined from the slope from the weight curve as a function of time divided by the cell area (3.8 $cm^2$). WVP was calculated as:

$$WVP = \frac{WVT\ e}{P_0\ RH}, \qquad (3)$$

where $e$ is the film thickness and $P_0$ is the saturation vapor pressure of water at room temperature. Assays were carried out in triplicate.

### *2.4.3 X-ray diffraction*

X-ray patterns of films were measured with a Malvern PANalytical Empyrean diffractometer (UK) using Cu (K-α) radiation (λ=1.54056 Å). Tests were performed in a 2θ range of 5 to 35° with a step size of 0.026°. Experiments were carried out in triplicate.

### *2.4.4 Fourier transform infrared spectroscopy*

FTIR analyses were performed using a Jasco FT-IR 4100 spectrometer (Japan) equipped with an attenuated total reflectance module (ATR, ZnSe crystal). Spectrums were recorded in a range from 4000 to 600 $cm^{-1}$ as the average of 64 scans with a resolution of 4 $cm^{-1}$. The spectra from starch films were normalized with respect to the 1149 $cm^{-1}$ peak, which is expected to not change with the incorporation of additives. Experiments were carried out in triplicate.

### *2.4.5 Thermogravimetric analysis*

Thermal properties were studied by thermogravimetric analysis (TGA, Shimadzu, Japan). Samples of 5 mg of each film were placed in aluminum pans in the TGA balance. Tests were performed under nitrogen atmosphere (flow rate of 30 mL/min) from 30 to 450 °C at a heat rate of 10 °C/min. Experiments were carried out in triplicate.

### *2.4.6 Mechanical properties*

Uniaxial tensile tests were performed using a Brookfield Texture Analyzer (CT3-100, USA) according to ASTM-D882-02 (2002). Probes of 35 mm x 5 mm x 0.2 mm (length, width and thickness, respectively) were tested at a strain rate of $10^{-3}$ $s^{-1}$. Representative curves of each system are presented, and Young modulus (E), stress at break ($\sigma_b$), strain at break ($\varepsilon_b$) and tensile toughness (T) values were calculated as the average of at least 10 measurements.

Dynamic Mechanical Thermal Analysis (DMTA) were carried out at 1 Hz at a heating rate of 2 °C/min from -80 to 40 °C using a DMTA IV (Rheometric Scientific, USA). Sample dimensions were 10 mm x 5 mm x 0.2 mm (length, width and thickness, respectively) and strain amplitude was fixed to 0.1 % so as to not exceed the elastic range. Tests were performed in triplicate.

### *2.4.7 Polyphenols content and antioxidant activity*

Polyphenols content was determined by Folin-Ciocalteu method. First, rosemary extract (0.1 g) was dissolved in 20 mL of ethanol:water mixture (70 % v/v) and sonicated for 20 min. Then, 400 µL of sample was mixed with 2 mL

of Folin-Ciocalteu reagent (1:10 diluted) and 1.6 mL of sodium carbonate (7 % w/v). Absorbance was measured at 760 nm after 30 min dark reaction using a spectrophotometer (Shimadzu UV-1800, Japan). The results were compared with a calibration curve performed with gallic acid (10-150 mg/L) and expressed as gallic acid equivalent per unit mass of the extract or the material (mg GAE/g). Determination was performed in triplicate.

Theoretical polyphenols content of films was calculated from the amount of extract incorporated and the polyphenols content of the extract.

The antioxidant activity of the rosemary extract and the films was measured using 1,1-diphenyl-2-picrylhydrazyl (DPPH•) reagent as a free radical. Film samples of 500 mg were immersed in 25 mL of hydrophilic (ethanol 10% v/v), lipophilic (ethanol 50% v/v) or acidic (3% acetic acid v/v) food simulants (European Commission, 2011) and placed in a shaker at 100 rpm for 24h. Then, an aliquot of 100 µL of each simulant or rosemary extract was mixed with 3.9 mL of DPPH• in methanol (25 mg/L), and absorbance was measured at 516 nm after 30 min reaction. Inhibition of DPPH free radicals was compared with a Trolox calibration curve (5–40 mM). Antioxidant activity of the rosemary extract was expressed as µmol Trolox equivalent (TE)/mg GAE and antioxidant activity of films was expressed as µmol Trolox equivalent (TE)/g of material. Assays were performed in triplicate.

### *2.4.8 Release kinetics*

Polyphenols release kinetics to the food simulants were studied. For this purpose, samples of 500 mg were immersed in 25 mL of hydrophilic (ethanol 10% v/v), lipophilic (ethanol 50% v/v) or acidic (3% acetic acid v/v) food simulants (European Commission, 2011) and placed in a shaker at 100 rpm. Aliquots of the supernatant (400 µL) were removed at different times from independent experiments and their polyphenols content was measured according to Folin-Ciocalteu methodology. Assays were performed in triplicate and the results were normalized with respect to the theoretical content and expressed as the percentage of released polyphenols as a function of time. Results were analyzed according to Weibull empirical model using SciPy (Oliphant, 2007).

In order to determine the contribution of the different release mechanisms, solubility and swelling of starch were studied. Solubility in food simulants was measured similarly to the description in Section 2.4.8. Swelling degree was measured according to Liu et al. (2017). Disks of 16 mm diameter were immersed in 30 mL of each food simulant. After 120 min, samples were removed and carefully wiped clear of excess liquid. Swelling degree was calculated as:

$$SD(\%) = 100 \times \frac{m_f}{m_0}, \quad (4)$$

where $m_0$ is the initial weight and $m_f$ is the weight of swollen sample. Assays were performed in triplicate.

### *2.4.8 Data processing and statistical analysis*

Data was analyzed using two-way ANOVA with 95% confidence level ($p < 0.05$) and Tukey post-hoc test. Results were reported as the mean and its standard deviation. “T” test was applied to compare results.

## 3. Results and discussion

### 3.1 Rosemary extract characteristics

A turbid solution was obtained when the powder extract was dispersed in water. Particles between 100 nm and 400 nm could be observed by SEM (Fig. 1a). Rosemary nanoparticles from a similar rosemary extract (ethanol 70%) diluted in water were obtained by solvent displacement method with diameters of (307 ± 33) nm (Estevez-Areco et al., 2018). In addition, López-Córdoba et al. (2017) produced rosemary nanoparticles by diluting a different rosemary extract (ethanol 96%) in water, obtaining particle diameters between 100 and 500 nm.

Chromatograms corresponding to the water soluble fraction or the ethanol soluble fraction are presented in Fig. 1b. Water soluble components were identified between 4 min and 6 min, while the rosemary nanoparticle components, which correspond to the ethanol soluble fraction, were mainly located between 6.5 min and 10 min. According to the literature, the more abundant molecules in rosemary extracts are rosmarinic acid, carnosol and carnosic acid (Herrero et al., 2010). Rosmarinic acid (5 min), carnosol (8 min) and carnosic acid (8.7 min) were identified according to their m/z ratio and their mass fragments. Polar components (shorter times) such as rosmarinic acid that were released to the aqueous medium will probably be miscible with the starch matrix. These molecules may interact with the polymer chains and act as plasticizers, as will be discussed in the next sections. On the other hand, non-polar molecules (larger times) such as carnosol or carnosic acid are forming the nanoparticles. A small fraction of polar components was also detected in the chromatogram of the rosemary nanoparticles.

The total polyphenol content of the rosemary extract resulted 290 mg GAE/g and the antioxidant activity resulted (7.5 ± 0.3) µmol TE/mg GAE. Recent researches reported an antioxidant activity of 3.39 µM TE/mg GAE for an aqueous rosemary extract (Martínez, Castillo, Ros, & Nieto, 2019) and 4.38 µmol TE/mg GAE for a rosemary extract obtained in an acetone/water/acetic acid solution (Fernandes et al., 2016). The rosemary extract obtained in this work showed higher antioxidant activity with respect to the consulted literature, which could be consequence of the extraction procedure and the rosemary leaves source.

a

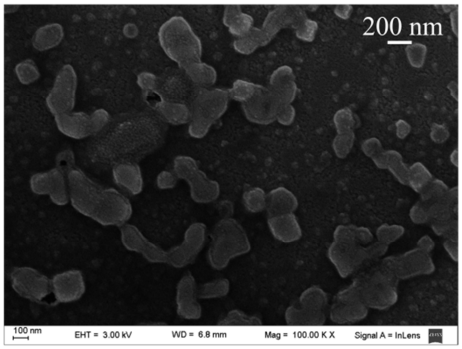


b

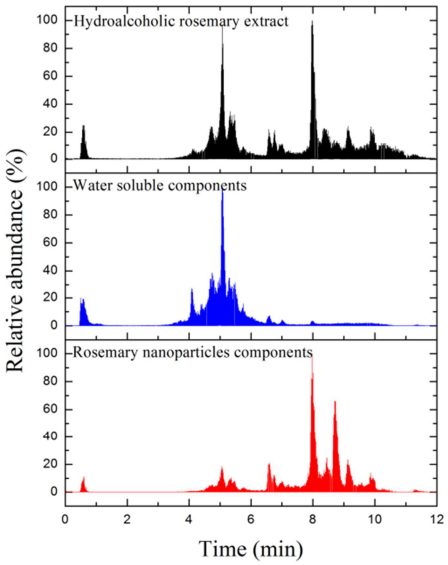

Figure 1: (a) SEM image of rosemary nanoparticles and (b) chromatograms corresponding to the hydroalcoholic rosemary extract, the water soluble components and the rosemary nanoparticles components.

### 3.2 Films morphology

SEM images of the films cryogenic fracture surfaces are shown in Fig. 2. Control film showed a smooth surface without the presence of pores, cracks or broken starch granules (Fig. 2a), suggesting a complete gelatinization after extrusion and thermo-compression processes, as reported by González-Seligra et al. (2017). Typical micrographs of nanocomposites were obtained for the films containing rosemary extract, in which spherical rosemary nanoparticles with diameters between 100 and 500 nm were located within the starch matrix. The nanoparticles were formed from the non-water soluble components, and their production occurred when the extract was incorporated into the water during the preparation of the mixtures before extrusion (Section 2.3.1). In the present research nanoparticles were conserved during extrusion process, showing that the mechanical and thermal energies involved in the process were not high enough to break them. Inset in Fig. 2b shows an image of S-R2.5 system with higher magnification. No holes were observed associated neither to detached nanoparticles nor between the nanoparticles and the matrix, and the particles are partially covered by the polymer. These effects indicate a good adhesion between matrix and particles. Nanoparticles were observed rather well dispersed in all the studied systems (Fig. 2a, 2b and 2c). Nevertheless, increasing rosemary extract concentration to 5% led some particles to agglomerate. This effect was increased when 10% of extract was incorporated. Particles and agglomerates were well distributed throughout the samples of these systems, as can been observed in SEM images with less magnification (Fig. 2e and 2f). López-Córdoba et al. (2017) have previously reported on the agglomeration of rosemary nanoparticles in starch films obtained by casting when the extract concentration was increased from 5% to 20% (w/w of filmogenic solution). In the present research, S-R10 films also showed a large amount of well dispersed particles, which could indicate that extrusion shear forces reduced agglutination of nanoparticles.

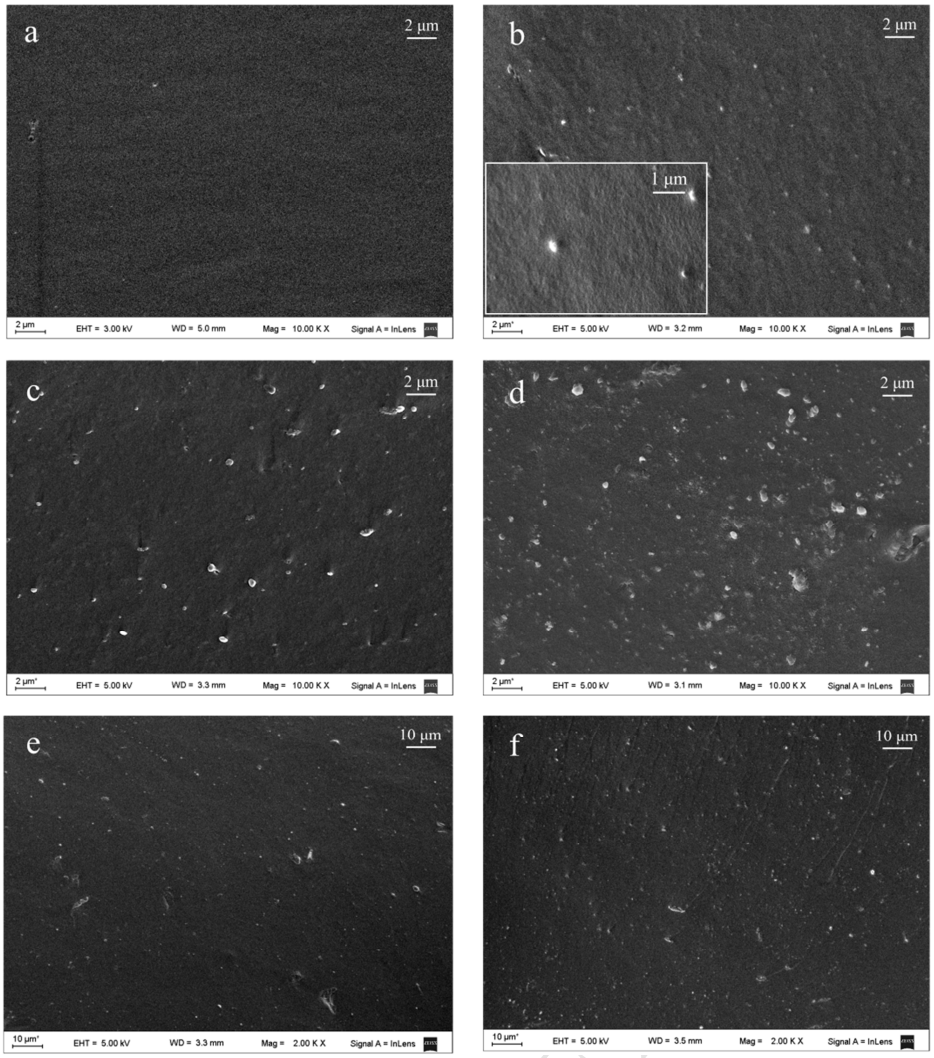


Figure 2: SEM micrographs (10 kx) of the cryogenic surfaces of Control (a), S-R2.5 (b), S-R5 (c), and S-R10 (d). Inset in b shows a rosemary nanoparticle image obtained with higher magnification (25 kx). No cracks or holes are observed, indicating a great adhesion. SEM micrographs of S-R5 (e) and S-R10 (f) with less magnification (2 kx) shows rather well dispersed nanoparticles throughout the samples.

### 3.3 Susceptibility to water

MC, WS and WVP values of the different films are presented in Table 2. Control, S-R2.5 and S-R5 films did not show significant differences in WVP. The presence of nanoparticles in a polymeric matrix increases the tortuous path by dispersing water molecules and thus decreasing their diffusion rate (Kuswandi, 2016). On the other hand, hydrophilic rosemary molecules could be miscible with the starch matrix and act as plasticizer. Plasticizers increase the free volume leading to an increase in the diffusion rate of water molecules (Marcilla & Beltran, 2004). The competition between both effects explains the observed behavior for WVP for the films with rosemary extract content up to 5%. However, a significant decrease in WVP was observed in the S-R10 system. This behavior could be associated with the increase in the concentration of rather well dispersed agglomerates of rosemary nanoparticles, as was discussed in the Section 3.2. López-Córdoba et al. (2017) showed that WVP increased in starch films obtained by casting with the incorporation of rosemary nanoparticles. This behavior was attributed to poor interfacial interactions between the nanoparticles and the polymer that favored the diffusion of water molecules. Nevertheless, in the present research a good adhesion between nanoparticles and starch phase was observed in the SEM micrographs (Section 3.2), possibly because the rosemary extract was performed

in an ethanol:water mixture (70:30 v/v) instead of in commercial grade ethanol (96%), as the extract of the cited research. The ethanol:water mixture extracted more polar components from rosemary leaves, which interact with both starch and nanoparticles, leading to a more continuous interphase. Oliveira, G.A.R., Oliveira, A.E., Conceição, & Leles (2016) showed that water soluble compounds, as rosmarinic acid, were extracted in significant larger amount in an ethanol:water mixture (70:30 v/v) with respect to commercial grade ethanol.

MC was not significantly affected by the rosemary extract concentration, while WS increased with rosemary extract content. The increase in the WS could be the consequence of the rosemary soluble compounds that were released into the water during the assays. Release of rosemary components will be discussed in Section 3.9.

Table 2: Susceptibility to water of the different films (MC, WS and WVP).

| Sample | MC (%) | WS (%) | WVP (g $m^{-1}$ $s^{-1}$ $Pa^{-1}$ x $10^{-10}$) |
|---|---|---|---|
| Control | $22 \pm 1^{a}$ | $19 \pm 1^{a}$ | $5.38 \pm 0.06^{a}$ |
| S-R2.5 | $23 \pm 1^{a}$ | $20 \pm 1^{ab}$ | $4.94 \pm 0.49^{a}$ |
| S-R5 | $24 \pm 2^{a}$ | $22 \pm 1^{b}$ | $4.63 \pm 0.79^{a}$ |
| S-R10 | $24 \pm 1^{a}$ | $25 \pm 1^{c}$ | $2.62 \pm 0.08^{b}$ |

Different letters within the same column indicate statistically significant differences ($p < 0.05$).

### 3.4 X-Ray Diffractometry

Figure 3 presents the X-ray diffraction patterns of the different samples. Control films showed a semicrystalline pattern with peaks centered at 12.9°, 14.9°, 16.8°, 18.3°, 19.7° and 22.1°. Diffraction peaks centered at 14.9°, 16.8° and 22.1° are related to B-structure, while peaks at 12.9°, 18.3° and 19.7° correspond to $V_h$ structure (Chanjarujit, Hongsprabhas, & Chaiseri, 2018; Van Soest, Hulleman, De Wit, & Vliegenthart, 1996). The presence of B-structure is mainly due to retrogradation of starch during storage, although there could be a contribution from some non-gelatinized granules (González-Seligra et al., 2017; Morales et al., 2015). On the other hand, $V_h$ crystals are usually formed during extrusion and consist of amylose forming complexes with glycerol (Buléon, Véronèse, & Putaux, 2007; Obiro, Sinha Ray, & Emmambux, 2012).

Similar diffraction patterns were observed in the films containing rosemary extract, but the 16.8°, 19.7° and 22.2° peaks widened and shifted about ~0.3° to higher angles, while the 18.4° peak shifted about ~0.2° to lower angles. These changes could be associated with the inclusion of some rosemary compound in the crystalline structure, which would modify the inter-planar spacing and deform the lattice, leading to the observed differences. Besides, the 18.2° peak of films containing rosemary extract showed higher intensity with respect to 18.4° peak of control samples. The increased relative height indicates a different structure factor, which could be associated with the presence of another molecule in the $V_h$ crystalls. Several studies have focused on the amylose property to form complexes with lipids, glycerol, butanol, isopropyl alcohol, flavor compounds, among other molecules (Buléon et al., 2007; Chanjarujit et al., 2018; Le Bail, Rondeau, & Buleon, 2005), but there is no available information about the complexation of amylose with any rosemary compound. In Fig. 3, it should also be noted that the shift in the 16.8° and 22.1° peaks was higher in the S-R2.5 system with respect to the S-R10 system, which could indicate that a greater deformation of the lattice occurred for low content of extract. More research must be carried out in order to determine the encapsulation of rosemary compounds by amylose.

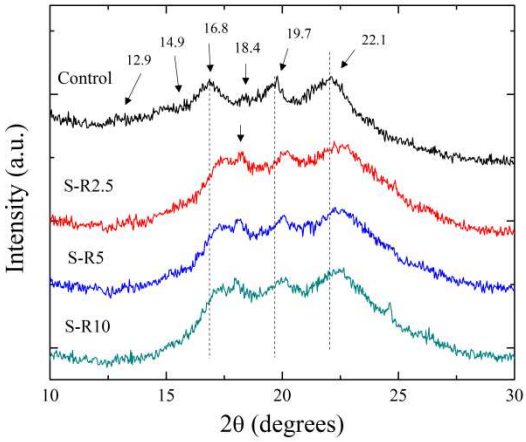


Figure 3: XRD patterns for the different films. Vertical dot lines show the shift of some crystalline peaks from starch with the incorporation of rosemary extract. The arrow in the S-R2.5 pattern points out the increment in the intensity of the 18.4° crystalline peak ($V_h$ structure).

### 3.5 Fourier-transform infrared spectroscopy

FTIR spectra of rosemary extract and the starch based films are shown in Fig. 4a. The rosemary spectrum showed characteristic bands associated with O-H stretching (3300 $cm^{-1}$), C-H stretching (2929 $cm^{-1}$), C=C ring stretching (1597 $cm^{-1}$), and C-O-H stretching in phenolic groups (1264 and 1029 $cm^{-1}$). Rosemary particles are formed by molecules with hydroxyl groups in their structure, such as carnosic acid, which allows them to interact with the different matrix components (starch, water, glycerol and/or rosemary water soluble components). These interactions would be responsible of the good adhesion between the particles and the matrix. Spectra of all the films showed the characteristic bands of starch corresponding to O-H stretching (3300 $cm^{-1}$), C-H stretching from alkyl groups (2927 $cm^{-1}$ and 2892 $cm^{-1}$), C-O and C-C stretching (1149 $cm^{-1}$ and 1077 $cm^{-1}$, respectively), and C-O-H bending (1100-900 $cm^{-1}$). In the films containing rosemary extract, the band of phenols centered at 1029 $cm^{-1}$ overlapped with C-O-H vibrations of starch, leading to an increase of the intensity of the 1022 $cm^{-1}$ band (Fig. 4b). No other characteristic band of rosemary extract or modifications of starch bands were observed. The absence of bands associated with phenolic groups was previously reported on starch-rosemary extract films made by casting (López-Córdoba et al., 2017), and in starch-chitosan films containing thyme extract (Talón, et al., 2017a). In both works, similar extract concentrations as those of the present work were used. FTIR seems to be not conclusive in determining the presence of a natural extract in a polymeric matrix, but it shows that rosemary extract does not modify starch during extrusion.

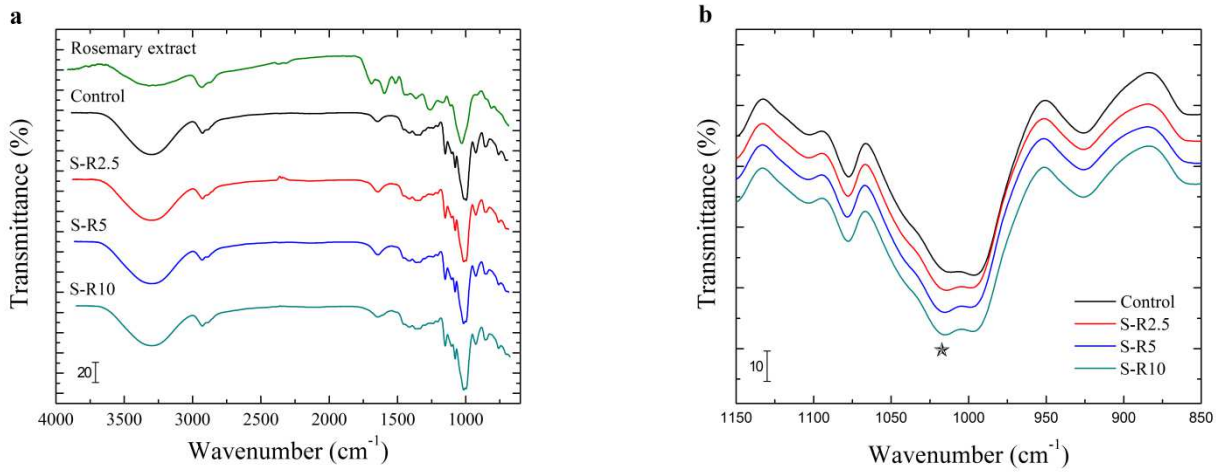


Figure 4: (a) Complete FTIR spectrum of the rosemary extract, the rosemary nanoparticles and the developed films, and (b) detail of the 1150-850 $cm^{-1}$ region, showing the increase in the 1022 $cm^{-1}$ peak height (✯).

### 3.6 Thermogravimetric analyses

TGA of starch based films and rosemary extract are shown in Fig. 5. The degradation of the extract begins at 170 °C and consists of two processes, as evidenced in the derivative curve. The first weight loss, located between 170 °C and 225 °C, corresponds to the loss of rosemary volatile compounds, while the second weight loss, located between 225 °C and 400 °C, is attributed to the decomposition of bioactive components (Cordeiro et al., 2013). In addition, the mass loss of 4% that occurred before 170 °C could be due to the evaporation of the remaining solvent (water and ethanol) in the extract. The thermal degradation of rosemary extract left a residual mass of ~45 % at 450 °C. The thermal stability of the extract suggests that there will be no significant loss of rosemary active compounds by thermal energy during extrusion, since the highest temperature of the process was 140 °C (Section 2.3.2).

Thermal degradation of starch films occurs in three steps, as previously reported by many authors (García, Ribba, Dufresne, Aranguren, & Goyanes, 2011; Wilhelm, Sierakowski, Souza, & Wypych, 2003). The first is located between 50 °C and 150 °C and corresponds to water evaporation. The second step is between 150 °C and 250 °C and is related to glycerol-rich phase degradation, while the third and main degradation step occurs from 250 °C to 340 °C and is attributed to starch-rich phase degradation. As evidenced in the derivative curve, starch degradation begins at lower temperatures on the films containing rosemary extract, suggesting that the presence of the rosemary components weakens the interactions between starch chains, favoring the hydrogen bonding between the hydroxyl groups from the starch and the polar compounds of the extract. Similar results were reported for starch casting films containing yerba mate extract (Medina Jaramillo, Gutiérrez, Goyanes, Bernal, & Famá, 2016), green tea extract (Medina-Jaramillo, Ochoa-Yepes, Bernal, & Famá, 2017), cocoa nibs extract (Kim, Baek, Go, & Song, 2018), and for starch films obtained by extrusion followed by thermo molding incorporating blueberry extract (Gutiérrez, & Alvarez, 2018). The residual mass at 450 °C increased with the content of rosemary extract because of the rosemary components that did not degrade.

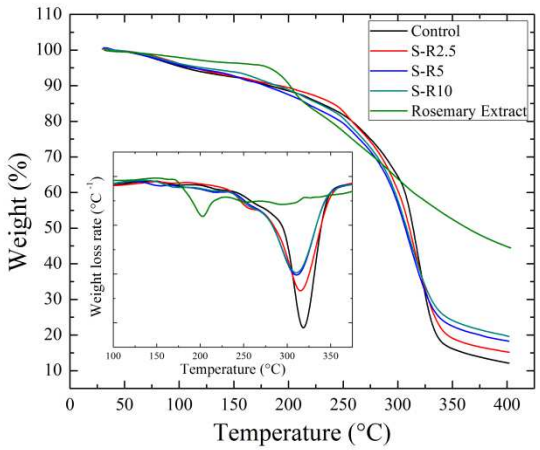


Figure 5: TGA curves of rosemary extract and different films. Derivative curves (inset) show clearly the shift to lower temperatures of the starch-rich phase degradation with the incorporation of rosemary extract.

### 3.7 Dynamic mechanical analysis

Fig. 6 presents the evolution of tan δ as a function of temperature of all films. Starch films plasticized with glycerol behave as a partially miscible system with two main relaxation processes, which are related to the presence of a glycerol-rich phase and a starch-rich phase (Morales et al., 2015). The low temperature process ($T_1$) is related to the glycerol-rich phase relaxation and it is centered at around -64 °C for control films, in agreement with the literature (Castillo et al., 2013; López, Lecot, Zaritzky, & García, 2011). This peak shifted to higher temperatures and widened with increasing the rosemary extract concentration. The incorporation of nanoparticles probably reduced the mobility of starch chains, introducing additional friction mechanisms (García et al., 2011), leading to the increase of the temperature and the widening of the transition. This effect was also observed for the starch-rich phase relaxation ($T_2$) in S-R2.5 system, which shifted from approximately 5°C towards higher temperatures. Besides, Fig. 5 showed that the starch-rich phase peak of S-R5 and S-R10 shifted to lower values with respect to S-R2.5 films. This behavior could indicate that some rosemary components acted as plasticizer of the starch-rich phase, compensating for the effect of the nanoparticles. Alternatively, a simultaneous increase in $T_1$ and decrease in $T_2$ could indicate that starch-rich and glycerol-rich phases were more miscible in S-R5 and S-R10 systems with respect to S-R2.5 system, since relaxation temperatures approached each other.

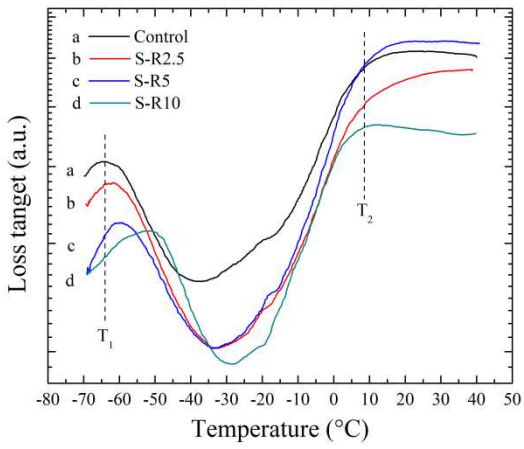

Figure 6: Loss tangent as a function of temperature for the different films. Vertical dot lines are centered in the transition temperatures of glycerol-rich phase ($T_1$) and starch-rich phase ($T_2$) of control film.

### 3.8 Uniaxial tensile behavior

Representative stress-strain curves are shown in Figure 7 and Young's modulus, stress at break, strain at break and tensile toughness are summarized in Table 3. All systems showed the typical behavior of thermoplastic starch films, consisting of a linear elastic deformation followed by a non-linear plastic behavior until failure. S-R2.5 showed a similar Young's modulus and higher stress and strain at break with respect to control films. On the other hand, S-R5 and S-R10 showed lower values of Young's modulus and stress at break with increasing rosemary extract content. Tensile toughness values were significantly higher for S-R 2.5 and S-R10. These results could be the consequence of two combined effects: the reinforcement caused by rosemary nanoparticles and the plasticizing effect of the miscible rosemary components. At a low concentration of extract, nanoparticles acted as well dispersed nanofillers, thus avoiding cracks propagation without lowering the Young's modulus (Morales et al., 2015). The nanoparticles agglutinated at higher concentrations generating a partial loss of their reinforcing effect. Miscible components of rosemary extract could act as plasticizer, which explains the observed lower Young's modulus in S-R5 and S-R10 systems. A plasticizer is a low molecular weight molecule that is able to interact with polymer chains, diminishing their interactions. In this sense, several natural extract were reported to act as plasticizer (Eskandarinia, Rafienia, Navid, & Agheb, 2018; Nouri & Nafchi, 2014; Rojhan & Nouri, 2013). The plasticizing effect became more evident in S-R10, which showed a significantly higher strain at break with respect to all the other samples.

López-Córdoba et al. (2017) reported that rosemary nanoparticles incorporated into casting starch films acted as reinforcement, leading to higher values of Young's modulus and stress at break regardless of the extract content. In that research, rosemary nanoparticles were obtained during solvent casting by replacing an amount of water with the ethanol based rosemary extract, thus the mechanical properties could also have been affected by the presence of ethanol. In the present research, rosemary extract was dried in order to avoid effects from the solution employed in the extraction process. Therefore, the observed mechanical properties are exclusively due to the incorporation of rosemary extract.

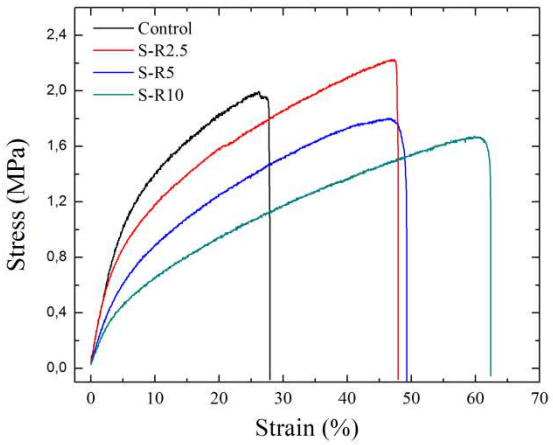


Figure 7: Stress-strain representative curves of the different films.

Table 3: Young's modulus (E), stress at break ($\sigma_b$), strain at break ($\varepsilon_b$) and tensile toughness (T).

| Sample | E (MPa) | $\sigma_b$ (MPa) | $\varepsilon_b$ (%) | T (kJ $m^{-3}$) |
|---|---|---|---|---|
| Control | 24.1 ± 1.8$^{a}$ | 2.01 ± 0.16$^{ab}$ | 30 ± 2$^{a}$ | 47 ± 7$^{a}$ |
| S-R2.5 | 23.3 ± 1.0$^{a}$ | 2.28 ± 0.25$^{b}$ | 50 ± 4$^{b}$ | 92 ± 8$^{b}$ |
| S-R5 | 14.8 ± 1.8$^{b}$ | 1.99 ± 0.24$^{ab}$ | 49 ± 5$^{b}$ | 65 ± 6$^{ab}$ |
| S-R10 | 9.3 ± 1.6$^{c}$ | 1.75 ± 0.25$^{a}$ | 70 ± 10$^{c}$ | 89 ± 13$^{b}$ |

Different letters within the same column indicate statistically significant differences ($p < 0.05$).

### 3.9 Polyphenols content and release

Table 4 presents the theoretical polyphenols content of the starch films, the maximum amount of released polyphenols to each food simulant obtained from the release experiments (Fig. 8). All the films were able to release more than 90% of theoretical polyphenols to hydrophilic and lipophilic food simulants. Particularly, the release to lipophilic medium resulted around 98% for S-R5 and S-R10, showing that no significant loss of polyphenols occurred during extrusion. For acidic food simulant, the maximum release of polyphenols was lower, reaching percentages between 76% and 87%. This lower release could be associated to lower polyphenols concentration as a result of lower solubility of rosemary active components in acidic medium (Wood, Senthilmohan, & Peskin, 2002).

The antioxidant activity of films immersed in food simulants is reported in Table 4. Nanocomposites with higher content of rosemary extract showed higher antioxidant activity in all simulants. Besides, the antioxidant activity did not show significant differences between the food simulants, indicating that most of the rosemary polyphenols maintained their activity despite the medium. However, the ratio between antioxidant activity and released polyphenols resulted higher for the lipophilic simulant. Several active components are only present in the ethanol soluble fraction of the rosemary extract (Section 3.1), such as carnosol and carnosic acid. These components could only be released in the lipophilic food simulant, which explains the higher antioxidant activity in this simulant.

Incorporation of natural extracts in polymeric films has been in the spotlight of many researches of active food packaging in recent years and several authors have incorporated rosemary extracts to biodegradable films. In particular, Gómez-Estaca, Bravo, Gómez-Guillén, Alemán, & Montero (2009) incorporated 2.5% or 20% of rosemary extract (w/v with respect to 4% gelatin solution) to bovine-hide gelatin films, and showed a scavenging activity of (3.67 ± 0.10) and (5.56 ± 0.09) mg of ascorbic acid equivalent/g film, respectively; Azevedo et al. (2019) added 0.08% (w/w with respect to solid phase) of rosemary essential oil to starch/whey protein isolate films, showing a DPPH scavenging activity of (87.90 ± 0.70)% when submerging 5 g of film in 5 mL of 80 % methanol; Bonilla & Sobral (2017) incorporated 1% of rosemary extract to gelatin/sodium caseinate films, and demonstrated an antioxidant activity of (4.31 ± 0.11) mM TE/g.

Table 4: Polyphenols theoretical content, maximum released polyphenols and antioxidant activity measured in food simulants after 1 day of release.

| Sample | Theoretical polyphenols content (mg GAE/g ) | Maximum released polyphenols released (mg GAE/g) | | | Antioxidant activity (µmol TE/g) | | |
|---|---|---|---|---|---|---|---|
| | | Hydrophilic | Lipophilic | Acid | Hydrophilic | Lipophilic | Acid |
| S-R2.5 | 4.28 ± 0.15$^{a}$ | 4.10 ± 0.02$^{a,1}$ | 4.01 ± 0.26$^{a,1}$ | 3.58 ± 0.32$^{a,1}$ | 33.6 ± 2.7$^{a,1}$ | 36.4 ± 3.5$^{a,1}$ | 29.5 ± 2.3$^{a,1}$ |
| S-R5 | 8.45 ± 0.30$^{b}$ | 7.84 ± 0.61$^{b,1}$ | 8.33 ± 0.12$^{b,1}$ | 6.39 ± 0.22$^{b,2}$ | 64.8 ± 3.4$^{b,1}$ | 81.4 ± 6.2$^{b,2}$ | 60.9 ± 5.8$^{b,1}$ |
| S-R10 | 16.43 ± 0.60$^{c}$ | 16.04 ± 0.39$^{c,1}$ | 16.13 ± 0.30$^{c,1}$ | 14.21 ± 0.80$^{c,2}$ | 123.1 ± 8.0$^{c,1}$ | 140.9 ± 8.8$^{c,2}$ | 134 ± 13$^{c,12}$ |

Different letters within the same column indicate statistically significant differences and different numbers within the same line indicate statistically significant differences ($p < 0.05$).

Release of polyphenols to different food simulants as a function of time is presented in Figure 8. For the hydrophilic food simulant (Fig.8a), release reached its maximum value in 100 min. A decrease of polyphenols was observed after 100 min, which could be associated with the oxidation of phenolic compounds (Talón, Trifkovic, Vargas, Chiralt, & González-Martínez, 2017b). A similar behavior was observed with the acidic food simulant (Fig. 8c), where the maximum release occurred at 240 min. In the lipophilic simulant, maximum release also occurred at 240 min for S-R2.5 and S-R5 systems, but for S-R10 occurred at 80 min (Fig. 8b). Release polyphenols remain constant in the lipophilic medium after the maximum release, which could be associated with slower oxidation kinetics in a lipophilic medium as consequence of lower $O_2$ diffusivity (Sada, Kito, Oda, & Ito, 1975) and with delayed release of some rosemary components that balanced the losses from oxidation. For example, rosemary nanoparticles are formed from components that are only soluble in ethanol (López-Córdoba et al., 2017), or water/ethanol mixtures, so it is expected that they can be released only in the lipophilic simulant.

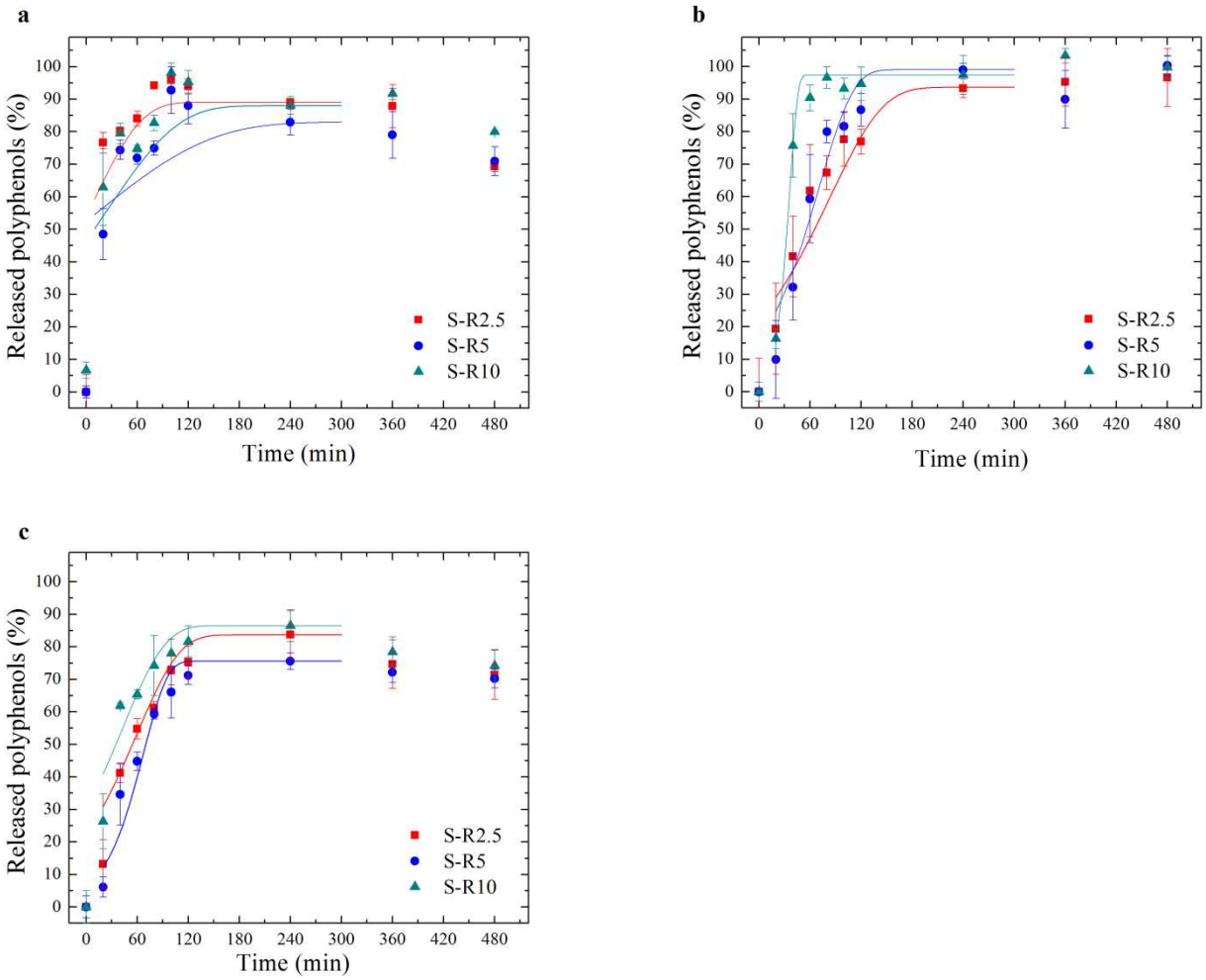


Figure 8: Percentage of polyphenols released to (a) hydrophilic, (b) lipophilic and (c) acid food simulants.

### 3.10 Release kinetics

Generally, the release of active compounds from a polymeric matrix is the consequence of several physical phenomena that occur simultaneously. For swellable systems, release is a coupling between diffusion and polymer chain relaxation (Ritger & Peppas, 1987), which is promoted by the diffusion of the solvent into the matrix. In a partially soluble system, like starch-glycerol, it is expected that active compounds will be released instantly as the matrix dissolves. A useful equation to model release kinetics is the Weibull function:

$$\frac{M_t}{M_\infty} = 1 - \exp(-a.b^t)\,, \qquad (5)$$

where $M_t$ is the amount of active compounds released at $t$ time, $M_\infty$ is the amount of active compounds released at equilibrium, and $a$ and $b$ are constants. Values of $b$ smaller than 0.75 indicate that Fickian diffusion is the leading mechanism of release, values between 0.75 and 1 indicate a Case II transport, and values higher than 1 indicate complex release mechanism (Papadopoulou, Kosmidis, Vlachou, & Macheras, 2006). The data obtained from the release kinetic experiments were fitted according to the Weibull equation and the results are presented in Table 4 and plotted in Fig. 8. Weibull model did not adjust well to the experimental data of hydrophilic medium, as can be observed in Fig. 8a. Values of $b$ parameter for all food simulants resulted higher than 1, indicating a complex release mechanism. A complex release mechanism implies that release rate does not change monotonically; it initially increases nonlinearly and after an inflection point it decreases asymptotically (Papadopoulou et al., 2006). Solubility of starch films resulted (22 ± 1)%, (18 ± 1)% and (20 ± 2)% for hydrophilic, lipophilic and acidic food simulants, respectively. According to these results, a similar amount of polyphenols was released in each medium as the matrix solubilizes, which contributed to the high initial release rate. At later times, other mechanisms such as diffusion or swelling rule the release. Swelling degree of films resulted (188 ± 3)%, (123 ± 3)% and (251 ± 5)% for hydrophilic, lipophilic and acid food simulants, respectively. Swelling in the acid medium resulted higher with respect to the hydrophilic medium, but polyphenols release was slower in this medium. On the other hand, the swelling degree in the lipophilic simulant resulted lower with respect to the acid medium but release was achieved at a similar rate in both simulants. A minimum swelling degree could induce polymer chain relaxation, promoting the polyphenols release (Liu et al., 2017); however, according to the results, swelling degree was not the determinant mechanism for polyphenols release kinetics in the studied systems. López-Córdoba et al. (2017) reported that starch films obtained by casting showed a significantly lower release rate of polyphenols to lipophilic simulant with respect to hydrophilic medium. However, in the cited research, an interaction between rosemary polyphenols and starch was observed by FTIR, which could slow down the release. As reported in Section 3.5, in the films developed by extrusion in this work there was no evidence of chemical interactions between polyphenols and starch, so a minimum swelling could easily promote the fast release of rosemary compounds.

According to the results of this research, starch active films cannot be used as a controlled release system when a high amount of water is available. Nevertheless, rosemary polyphenols that were successfully incorporated in the starch matrix during extrusion maintained their activity and could be released to several food simulants.

Table 5: Adjustment parameters of the release curves using Weibull model.

| | | Weibull equation | | |
|---|---|---|---|---|
| | | a | b | $R^2$ |
| S-R2.5 | Hydrophilic | $0.924 \pm 0.121^{a}$ | $1.017 \pm 0.003^{a}$ | 0.88 |
| | Lipophilic | $0.270 \pm 0.140^{b}$ | $1.016 \pm 0.005^{ab}$ | 0.81 |
| | Acid | $0.318 \pm 0.068^{b}$ | $1.018 \pm 0.003^{a}$ | 0.93 |
| S-R5 | Hydrophilic | $0.999 \pm 0.250^{a}$ | $1.007 \pm 0.004^{b}$ | 0.80 |
| | Lipophilic | $0.175 \pm 0.120^{bc}$ | $1.025 \pm 0.008^{a}$ | 0.94 |
| | Acid | $0.085 \pm 0.035^{c}$ | $1.037 \pm 0.006^{c}$ | 0.94 |
| S-R10 | Hydrophilic | $0.750 \pm 0.234^{a}$ | $1.012 \pm 0.005^{b}$ | 0.85 |
| | Lipophilic | $0.022 \pm 0.011^{d}$ | $1.111 \pm 0.020^{d}$ | 0.99 |
| | Acid | $0.431 \pm 0.135^{b}$ | $1.019 \pm 0.005^{a}$ | 0.88 |

Different letters within the same column indicate statistically significant differences ($p < 0.05$).

## 4. Conclusions

Nanocomposite starch films with high antioxidant activity were successfully obtained through extrusion process without having to encapsulate the active compounds. The activity of the polyphenols was conserved throughout the extrusion process due to the thermal stability of the rosemary extract. Besides, rosemary nanoparticles could resist the shear forces and were well dispersed within the matrix at low concentrations.

Rosemary polyphenols incorporated to the films were successfully released to hydrophilic, lipophilic and acidic simulants in less than 240 min, and similar antioxidant activity was achieved in all the media. The observed fast release of polyphenols was promoted by solubility, swelling and the absence of interactions between polyphenols and starch.

Incorporation of 2.5% (w/w) of rosemary extract led to films with higher stress and strain at break, without decreasing Young's modulus. The addition of 5% or 10% of rosemary extract led to films with lower Young's modulus and stress at break. However, in all cases the nanocomposites showed a tensile toughness between 38% and 96% higher than that of thermoplastic starch. Mechanical behavior was attributed to a competition between the nanoparticle reinforcement and the plasticizing effect of some rosemary miscible components.

## Acknowledgements

We thank Dr. Elsa López Loveira (3ia – UNSAM) for assistance withHPLC-MS measurements and Ms A. C. T. Kugler for her help in English revision.

## Fundings

This work was supported by Agencia Nacional de Promoción científica y Tecnológica (ANPCyT PICT 2017-2362), Secretaría de Política Universitarias (SPU 2017-2018 nro 1655), Universidad de Buenos Aires (UBACyT 20020170100381BA).

Declarations of interest: none.

## References

American Society for Testing and Materials. (2002). ASTM D882-02. In *Annual Book of ASTM.* West Conshohocken, PA: American Society for Testing and Materials.

Azevedo, V. M., Carvalho, R. A., Borges, S. V., Claro, P. I. C., Hasegawa, F. K., Yoshida, M. I., & Marconcini, J. M. (2019). Thermoplastic starch/whey protein isolate/rosemary essential oil nanocomposites obtained by extrusion process: Antioxidant polymers. *Journal of Applied Polymer Science, 136*(23), 47619. https://doi.org/10.1002/app.47619.

Bonilla, J., & Sobral, P. J. A. (2017). Antioxidant and physicochemical properties of blended films based on gelatin-sodium caseinate activated with natural extracts. *Journal of Applied Polymer Science*, *134*(7), 44467. https://doi.org/10.1002/app.44467.

Buléon, A., Véronèse, G., & Putaux, J.-L. (2007). Self-association and crystallization of amylose. *Australian Journal of Chemistry*, *60*(10), 706–718. https://doi.org/10.1071/CH07168.

Castillo, L., López, O., López, C., Zaritzky, N., García, M. A., Barbosa, S., & Villar, M. (2013). Thermoplastic starch films reinforced with talc nanoparticles. *Carbohydrate Polymers*, *95*(2), 664–674. https://doi.org/10.1016/j.carbpol.2013.03.026.

Cazón, P., Velazquez, G., Ramírez, J. A., & Vázquez, M. (2017). Polysaccharide-based films and coatings for food packaging: A review. *Food Hydrocolloids*, *68*, 136–148. https://doi.org/10.1016/j.foodhyd.2016.09.009.

Chanjarujit, W., Hongsprabhas, P., & Chaiseri, S. (2018). Physicochemical properties and flavor retention ability of

alkaline calcium hydroxide-mungbean starch films. *Carbohydrate Polymers*, *198*, 473–480. https://doi.org/10.1016/j.carbpol.2018.06.118.

Cordeiro, A., Medeiros, M. L., Santos, N. A., Soledade, L. E. B., Pontes, L., Souza, A. L., Queiroz, N., Souza, A. G. (2013). Rosemary (Rosmarinus officinalis L.) extract. *Journal of Thermal Analysis and Calorimetry*, *113*(2), 889–895. https://doi.org/10.1007/s10973-012-2778-4.

Cunniff, P. A., & Jee, M. H. (1995). Official Methods of Analysis of AOAC International (16th edn). *Trends in Food Science and Technology*, *6*(11), 382. ISSN 0924-2244.

Domínguez, R., Barba, F. J., Gómez, B., Putnik, P., Kovačević, D. B., Pateiro, M., Santos, E.M., Lorenzo, J. M. (2018). Active packaging films with natural antioxidants to be used in meat industry: A review. *Food Research International*, *113*, 93–101. https://doi.org/10.1016/j.foodres.2018.06.073.

dos Santos Caetano, K., Lopes, N. A., Costa, T. M. H., Brandelli, A., Rodrigues, E., Flôres, S. H., & Cladera-Olivera, F. (2018). Characterization of active biodegradable films based on cassava starch and natural compounds. *Food Packaging and Shelf Life*, *16*, 138–147. https://doi.org/10.1016/j.fpsl.2018.03.006.

Eskandarinia, A., Rafienia, M., Navid, S., & Agheb, M. (2018). Physicochemical, Antimicrobial and Cytotoxic Characteristics of Corn Starch Film Containing Propolis for Wound Dressing. *Journal of Polymers and the Environment, 26*(8), 3345-3351. https://doi.org/10.1007/s10924-018-1216-5.

Estevez-Areco, S., Guz, L., Candal, R., & Goyanes, S. (2018). Release kinetics of rosemary (Rosmarinus officinalis) polyphenols from polyvinyl alcohol (PVA) electrospun nanofibers in several food simulants. *Food Packaging and Shelf Life*, *18*, 42-50. https://doi.org/10.1016/j.fpsl.2018.08.006.

European Commission. (2011). Commission Regulation (EU) No 10/2011 on plastic materials and articles intended to come into contact with food. *Offical Journal of the European Union*, Vol. 15, pp. 12–88. https://doi.org/10.1016/j.nucengdes.2011.01.052.

Feng, M., Yu, L., Zhu, P., Zhou, X., Liu, H., Yang, Y., Zhou, J., Gao, C., Bao, X., Chen, P. (2018). Development and preparation of active starch films carrying tea polyphenol. *Carbohydrate Polymers*, *196*, 162–167. https://doi.org/10.1016/j.carbpol.2018.05.043.

Fernandes, R. de P. P., Trindade, M. A., Tonin, F. G., Lima, C. G. de, Pugine, S. M. P., Munekata, P. E. S., Lorenzo, J.M., De Melo, M. P. (2016). Evaluation of antioxidant capacity of 13 plant extracts by three different methods: cluster analyses applied for selection of the natural extracts with higher antioxidant capacity to replace synthetic antioxidant in lamb burgers. *Journal of Food Science and Technology*, *53*(1), 451–460. https://doi.org/10.1007/s13197-015-1994-x.

García, N. L., Famá, L., D'Accorso, N. B., & Goyanes, S. (2015). Biodegradable starch nanocomposites. In V. K. Thakur, & M. K. Thakur (Eds.), *Eco-friendly polymer nanocomposites* (pp. 17–77). Springer. https://doi.org/10.1007/978-81-322-2470-9_2.

García, N. L., Ribba, L., Dufresne, A., Aranguren, M., & Goyanes, S. (2011). Effect of glycerol on the morphology of nanocomposites made from thermoplastic starch and starch nanocrystals. *Carbohydrate Polymers*, *84*(1), 203–210. https://doi.org/10.1016/j.carbpol.2010.11.024.

Gómez-Estaca, J., Bravo, L., Gómez-Guillén, M. C., Alemán, A., & Montero, P. (2009). Antioxidant properties of tuna-skin and bovine-hide gelatin films induced by the addition of oregano and rosemary extracts. *Food Chemistry*, *112*(1), 18–25. https://doi.org/10.1016/j.foodchem.2008.05.034.

González-Seligra, P., Guz, L., Ochoa-Yepes, O., Goyanes, S., & Famá, L. (2017). Influence of extrusion process conditions on starch film morphology. *LWT-Food Science and Technology*, *84*, 520–528. https://doi.org/10.1016/j.lwt.2017.06.027.

Gutiérrez, T. J., & Alvarez, V. A. (2018). Bionanocomposite films developed from corn starch and natural and modified nano-clays with or without added blueberry extract. *Food Hydrocolloids, 77*, 407-420. https://doi.org/10.1016/j.foodhyd.2017.10.017.

Gutiérrez, T. J., Herniou-Julien, C., Álvarez, K., & Alvarez, V. A. (2018). Structural properties and in vitro digestibility of edible and pH-sensitive films made from guinea arrowroot starch and wastes from wine manufacture. *Carbohydrate Polymers*, *184*, 135–143. https://doi.org/10.1016/j.carbpol.2017.12.039.

Guz, L., Famá, L., Candal, R., & Goyanes, S. (2017). Size effect of ZnO nanorods on physicochemical properties of plasticized starch composites. *Carbohydrate Polymers*, *157*, 1611–1619. https://doi.org/10.1016/j.carbpol.2016.11.041.

Herrero, M., Plaza, M., Cifuentes, A., & Ibáñez, E. (2010). Green processes for the extraction of bioactives from Rosemary: Chemical and functional characterization via ultra-performance liquid chromatography-tandem mass spectrometry and in-vitro assays. *Journal of Chromatography A*, *1217*(16), 2512–2520. https://doi.org/10.1016/j.chroma.2009.11.032.

Iamareerat, B., Singh, M., Sadiq, M. B., & Anal, A. K. (2018). Reinforced cassava starch based edible film incorporated with essential oil and sodium bentonite nanoclay as food packaging material. *Journal of Food Science and Technology*, *55*(5), 1953–1959. https://doi.org/10.1007/s13197-018-3100-7.

Ji, Z., Yu, L., Liu, H., Bao, X., Wang, Y., & Chen, L. (2017). Effect of pressure with shear stress on gelatinization of starches with different amylose/amylopectin ratios. *Food Hydrocolloids*, *72*, 331–337. https://doi.org/10.1016/j.foodhyd.2017.06.015.

Khaneghah, A. M., Hashemi, S. M. B., & Limbo, S. (2018). Antimicrobial agents and packaging systems in antimicrobial active food packaging: An overview of approaches and interactions. *Food and Bioproducts Processing*, *111*, 1-19. https://doi.org/10.1016/j.fbp.2018.05.001.

Kim, S., Baek, S. K., Go, E., & Song, K. (2018). Application of Adzuki Bean Starch in Antioxidant Films Containing Cocoa Nibs Extract. *Polymers, 10*(11), 1210. https://doi.org/10.3390/polym10111210.

Kuswandi, B. (2016). Nanotechnology in Food Packaging. In S. Ranjan, N. Dasgupta, & E. Lichtfouse (Eds.), *Nanoscience in Food and Agriculture 1* (pp. 151–183). Springer. https://doi.org/10.1007/978-3-319-39303-2_6.

Le Bail, P., Rondeau, C., & Buleon, A. (2005). Structural investigation of amylose complexes with small ligands: helical conformation, crystalline structure and thermostability. *International Journal of Biological Macromolecules*, *35*(1–2), 1–7. https://doi.org/10.1016/j.ijbiomac.2004.09.001.

Liu, F., Avena-Bustillos, R. J., Chiou, B.-S., Li, Y., Ma, Y., Williams, T. G., Wood, D.F., McHugh, T.H., Zhong, F. (2017). Controlled-release of tea polyphenol from gelatin films incorporated with different ratios of free/nanoencapsulated tea polyphenols into fatty food simulants. *Food Hydrocolloids*, *62*, 212–221. https://doi.org/10.1016/j.foodhyd.2016.08.004.

López-Córdoba, A., Medina-Jaramillo, C., Piñeros-Hernandez, D., & Goyanes, S. (2017). Cassava starch films containing rosemary nanoparticles produced by solvent displacement method. *Food Hydrocolloids*, *71*, 26–34. https://doi.org/10.1016/j.foodhyd.2017.04.028.

López, O. V, Lecot, C. J., Zaritzky, N. E., & García, M. A. (2011). Biodegradable packages development from starch based heat sealable films. *Journal of Food Engineering*, *105*(2), 254–263. https://doi.org/10.1016/j.jfoodeng.2011.02.029.

Marcilla, A., & Beltran, M. (2004). Mechanisms of plasticizers action. In G. Wypych (Ed.), *Handbook of Plasticizers (pp.* 107–120). ChemTec Publishing. ISBN 978-1-895198-97-3.

Martínez, L., Castillo, J., Ros, G., & Nieto, G. (2019). Antioxidant and Antimicrobial Activity of Rosemary, Pomegranate and Olive Extracts in Fish Patties. *Antioxidants*, *8*(4), 86. https://doi.org/10.3390/antiox8040086.

Medina Jaramillo, C. M., Gutiérrez, T. J., Goyanes, S., Bernal, C., & Famá, L. (2016). Biodegradability and plasticizing effect of yerba mate extract on cassava starch edible films. *Carbohydrate Polymers*, *151*, 150–159. https://doi.org/10.1016/j.carbpol.2016.05.025 .

Medina-Jaramillo, C., Ochoa-Yepes, O., Bernal, C., & Famá, L. (2017). Active and smart biodegradable packaging based on starch and natural extracts. *Carbohydrate Polymers*, *176*, 187–194. https://doi.org/10.1016/j.carbpol.2017.08.079.

Morales, N. J., Candal, R., Famá, L., Goyanes, S., & Rubiolo, G. H. (2015). Improving the physical properties of starch using a new kind of water dispersible nano-hybrid reinforcement. *Carbohydrate Polymers*, *127*, 291–299. https://doi.org/10.1016/j.carbpol.2015.03.071.

Nouri, L., & Nafchi, A. M. (2014). Antibacterial, mechanical, and barrier properties of sago starch film incorporated with betel leaves extract. *International Journal of Biological Macromolecules*, *66*, 254–259. https://doi.org/10.1016/j.ijbiomac.2014.02.044.

Obiro, W. C., Sinha Ray, S., & Emmambux, M. N. (2012). V-amylose structural characteristics, methods of preparation, significance, and potential applications. *Food Reviews International*, *28*(4), 412–438. https://doi.org/10.1080/87559129.2012.660718.

Ochoa-Yepes, O., Di Giogio, L., Goyanes, S., Mauri, A., & Famá, L. (2019). Influence of process (extrusion/thermo-compression, casting) and lentil protein content on physicochemical properties of starch films. *Carbohydrate Polymers, 208*, 221-231. https://doi.org/10.1016/j.carbpol.2018.12.030.

Oliphant, T. E. (2007). SciPy: Open source scientific tools for Python. *Computing in Science and Engineering*, *9*, 10–20. https://doi.org/10.1109/MCSE.2007.58.

Oliveira, G. A. R., Oliveira, A. E., Conceição, E. C., & Leles, M. I. G. (2016). Multiresponse optimization of an extraction procedure of carnosol and rosmarinic and carnosic acids from rosemary. *Food Chemistry*, *211*, 465–473. https://doi.org/10.1016/j.foodchem.2016.05.042.

Ortega-Toro, R., Collazo-Bigliardi, S., Roselló, J., Santamarina, P., & Chiralt, A. (2017). Antifungal starch-based edible films containing Aloe vera. *Food Hydrocolloids*, *72*, 1–10. https://doi.org/10.1016/j.foodhyd.2017.05.023.

Papadopoulou, V., Kosmidis, K., Vlachou, M., & Macheras, P. (2006). On the use of the Weibull function for the discernment of drug release mechanisms. *International Journal of Pharmaceutics*, *309*(1–2), 44–50. https://doi.org/10.1016/j.ijpharm.2005.10.044.

Piñeros-Hernandez, D., Medina-Jaramillo, C., López-Córdoba, A., & Goyanes, S. (2017). Edible cassava starch films carrying rosemary antioxidant extracts for potential use as active food packaging. *Food Hydrocolloids*, *63*, 488–495. https://doi.org/10.1016/j.foodhyd.2016.09.034.

Ritger, P. L., & Peppas, N. A. (1987). A simple equation for description of solute release II. Fickian and anomalous release from swellable devices. *Journal of Controlled Release*, *5*(1), 37–42. https://doi.org/10.1016/0168-3659(87)90035-6.

Rojhan, M., & Nouri, L. (2013). Antimicrobial, Physicochemical, Mechanical, and Barrier Properties of Tapioca Starch Films Incorporated with Eucalyptus Extract. *Journal of Chemical Health Risks*, *3*(3), 43-52. https://doi.org/ 10.22034/JCHR.2018.544037.

Sada, E., Kito, S., Oda, T., & Ito, Y. (1975). Diffusivities of gases in binary mixtures of alcohols and water. *The Chemical Engineering Journal*, *10*(1), 155–159. https://doi.org/10.1016/0300-9467(75)88030-0.

Shah, U., Naqash, F., Gani, A., & Masoodi, F. A. (2016). Art and science behind modified starch edible films and coatings: a review. *Comprehensive Reviews in Food Science and Food Safety*, *15*(3), 568–580. https://doi.org/10.1111/1541-4337.12197.

Talón, E., Trifkovic, K. T., Nedovic, V. A., Bugarski, B. M., Vargas, M., Chiralt, A., & González-Martínez, C. (2017a). Antioxidant edible films based on chitosan and starch containing polyphenols from thyme extracts. *Carbohydrate Polymers*, *157*, 1153–1161. https://doi.org/10.1016/j.carbpol.2016.10.080.

Talón, E., Trifkovic, K. T., Vargas, M., Chiralt, A., & González-Martínez, C. (2017b). Release of polyphenols from starch-chitosan based films containing thyme extract. *Carbohydrate Polymers*, *175*, 122–130. https://doi.org/10.1016/j.carbpol.2017.07.067.

Toro-Márquez, L. A., Merino, D., & Gutiérrez, T. J. (2018). Bionanocomposite films prepared from corn starch with and without nanopackaged Jamaica (Hibiscus sabdariffa) flower extract. *Food and Bioprocess Technology*, *11*(11), 1955–1973. https://doi.org/10.1007/s11947-018-2160-z.

Van Soest, J. J. G., Hulleman, S. H. D., De Wit, D., & Vliegenthart, J. F. G. (1996). Crystallinity in starch bioplastics. *Industrial Crops and Products*, *5*(1), 11–22. https://doi.org/10.1016/0926-6690(95)00048-8.

Vilela, C., Kurek, M., Hayouka, Z., Röcker, B., Yildirim, S., Antunes, M. D. C., Nilsen-Nygaard, J., Pettersen, M.K. Freire, C. S. R. (2018). A concise guide to active agents for active food packaging. *Trends in Food Science & Technology*, *80,* 212-222. https://doi.org/10.1016/j.tifs.2018.08.006.

Wilhelm, H.-M., Sierakowski, M.-R., Souza, G. P., & Wypych, F. (2003). Starch films reinforced with mineral clay. *Carbohydrate Polymers*, *52*(2), 101–110. https://doi.org/10.1016/S0144-8617(02)00239-4.

Wood, J. E., Senthilmohan, S. T., & Peskin, A. V. (2002). Antioxidant activity of procyanidin-containing plant extracts at different pHs. Food Chemistry, 77(2), 155-161. https://doi.org/10.1016/S0308-8146(01)00329-6.

Yildirim, S., Röcker, B., Pettersen, M.K., Nilsen-Nygaard, J., Ayhan, Z., Rutkaite R., Radusin, T., Suminska , P., Marcos, B., Coma, V. (2018). Active packaging applications for food. *Comprehensive Reviews in Food Science and Food Safety*, *17*(1), 165-199. https://doi.org/10.1016/B978-0-323-51271-8.00007-3.

Web references

Morales, J., Morgan, M., Palmer, A. *A sea change: Plastics Pathway to Sustainability Special Report*. IHS Markit (2018). https://ihsmarkit.com/products/sea-plastics-pathway.html

US Food & Drug Administration. FDA cite: 21CFR182.20. (2018). https://www.accessdata.fda.gov/scripts/cdrh/cfdocs/cfcfr/CFRSearch.cfm?fr=182.20.

**Highlights**

- Bioactive nanocomposite starch films containing rosemary extract were developed by extrusion
- Rosemary extract maintained its antioxidant activity after extrusion
- Most of rosemary polyphenols were released to several food simulants
- Low extract concentration increased stress and strain at break
- High concentration lowered Young's modulus and stress at break